Magnetic behavior of single-crystalline Pr_5Ge_3 and Tb_5Ge_3 compounds

Devang A. Joshi, A. Thamizhavel, and S. K. Dhar
Department of Condensed Matter Physics and Material Sciences, Tata Institute of Fundamental Research, Homi Bhaba Road, Colaba, Mumbai 400 005, India

(Received 24 September 2008; published 21 January 2009)

The results of the magnetization studies on Pr_5Ge_3 and Tb_5Ge_3 single crystals are reported. Single crystals of Pr_5Ge_3 and Tb_5Ge_3 compounds were successfully grown by Czochralski method. These compounds crystallize in a Mn_5Si_3-type hexagonal structure with space group $P6_3/mcm$. Ferromagnetic correlations set in at around 36 K in Pr_5Ge_3 in the *ab* plane followed by an antiferromagnetic transition at 13 K. Along the *c* axis the magnetization shows a ferromagnetic transition around 13 K with an overall ferrimagnetic behavior. At 2 K, the magnetic isotherm of the compound along the [0001] direction is typical for a ferromagnet, while a field-induced ferromagneticlike response is observed along the $[10\bar{1}0]$ direction. The hexagonal *ab* plane or $[10\bar{1}0]$ direction was found to be the easy axis of magnetization. Tb_5Ge_3 orders antiferromagnetically at 85 K with a hexagonal *ab* plane as the easy axis of magnetization. The compound shows a field-induced ferromagnetic behavior in its magnetic isotherm at 2 K.

DOI: 10.1103/PhysRevB.79.014425 PACS number(s): 71.20.Eh, 71.27.+a

I. INTRODUCTION

R_5M_3 (R=rare earths and $M=p$ block elements) compounds exist for a variety of M elements such as M=Si, Ge, Ga, Pb, and Sn. The crystal structure of these binary compounds depends upon the atomic sizes of R and M as well as the type of the p block element. Most of the R_5M_3 crystallize in the Mn_5Si_3-type hexagonal structure in which the rare-earth atoms occupy two inequivalent crystallographic 4*d* and 6*g* sites located at (1/3, 2/3, 0) and (x_R,0,1/4). Due to the different near-neighbor environment associated with the two sites, R_5M_3 compounds typically show complicated magnetic structures despite their relatively simple formula. A variety of behaviors such as the coexistence of antiferromagnetic and ferromagnetic components, incommensurate amplitude modulated and conical spin structures, and field-induced magnetic configurations are observed. The R_5Ge_3 family of compounds was first studied by Buschow and Fast[1] using polycrystalline materials. Bulk magnetization indicates that Ce_5Ge_3 and Nd_5Ge_3 are ferrimagnetic; Pr_5Ge_3, Tb_5Ge_3, Dy_5Ge_3, Ho_5Ge_3, and Er_5Ge_3 are weak antiferromagnets at low temperature and exhibit a field-induced metamagnetic transition.[1] A neutron-diffraction study on Nd_5Ge_3 (Ref. 2) was more revealing and the results could best be explained by assuming a collinear antiferromagnetic double sheet structure for the Nd atoms at the 6*g* site and a canted (or a possible modulated) structure for the 4*d* atoms. Below 20 K a fairly strong ferromagnetic component can be induced by means of an external field in Nd_5Ge_3.

There are very few reports based on single crystals of R_5Ge_3. A single crystal of Ce_5Ge_3 was reported to show dense Kondo behavior.[3] Tsutaoka *et al.* reported the magnetization and electrical transport properties of single crystals of Gd_5Ge_3 and Tb_5Ge_3.[4] Gd_5Ge_3 undergoes two antiferromagnetic transitions at 76 and 52 K, respectively, while a single antiferromagnetic transition at 79 K and a large magnetic anisotropy are observed in Tb_5Ge_3. Keeping in mind the complicated magnetic behavior of Nd_5Ge_3 in the ordered state, we have been motivated to examine the corresponding behavior in a single-crystal specimen of the neighboring Pr_5Ge_3. The large magnetic anisotropy in Tb_5Ge_3 prompted us to study its magnetization behavior in greater detail than that given in Ref. 4. Accordingly, we have successfully grown single crystals of Pr_5Ge_3 and Tb_5Ge_3, and the results of our magnetization study are presented in this paper.

II. EXPERIMENT

From the phase diagram of the Pr-Ge and Tb-Ge systems, Pr_5Ge_3 and Tb_5Ge_3 were found to be congruently melting with a melting point of 1490 and 1900 °C, respectively. Taking the advantage of this property, we decided to grow both the single crystals by Czochralski pulling method. Starting materials were high-purity Pr (99.95 %) and Ge (99.999%) metals from Leico industries. Stoichiometric amount of materials was taken to make a 10 g (polycrystal) melt in a tetra-arc furnace. A thin polycrystalline seed rod of the respective compound was immersed into the melt and pulled at a speed of 10 mm/h in pure and dry argon atmosphere. The as-grown ingot was approximately 2–3 mm in diameter and 6 cm in length.

The phase homogeneity of the crystal was checked using the powder x-ray diffraction. The single crystals were oriented along the principle crystallographic directions using back-reflection Laue diffraction method and then cut to the required size for thermal and magnetic measurements. The magnetic measurements were performed using superconducting quantum interference device (SQUID) (Quantum Design) and vibrating sample magnetometer (VSM) (Oxford Instruments) within a temperature range of 1.8–300 K and magnetic fields up to 120 kOe. The heat-capacity measurement was performed using a physical property measurement system (PPMS) (Quantum Design).

III. RESULT

As mentioned in Sec. I, both Pr_5Ge_3 and Tb_5Ge_3 form in Mn_5Si_3-type hexagonal structure with space group $P6_3/mcm$

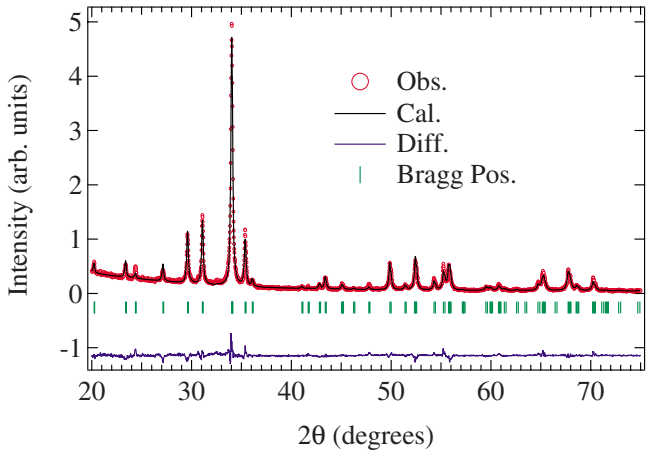

FIG. 1. (Color online) Rietveld analysis of the x-ray powder pattern of the Pr_5Ge_3 compound.

(No. 193). In order to confirm the phase homogeneity of the compounds with proper crystallographic and lattice parameters, a Rietveld analysis of the observed x-ray pattern was done using the FULLPROF program as shown in Fig. 1. The single-phase nature of the samples was also confirmed by scanning electron microscopy (SEM). The lattice parameters obtained from the Rietveld analysis for Pr_5Ge_3 and Tb_5Ge_3 are $a=8.804$ Å, $c=6.588$ Å and $a=8.474$ Å, $c=6.305$ Å, respectively. The lattice parameters are in close agreement with the reported ones.[1] The refined crystallographic parameters for Pr_5Ge_3 are presented in Table I, and the crystal structure is shown in Fig. 2. The black line edges represent a unit cell consisting of 2 f.u. of Pr_5Ge_3. The *xy* planes on the top, bottom, and middle which consist of only Pr atoms labeled as Pr1 represent the crystallographic 4*d* planes. The remaining two planes which consist of both Pr (labeled as Pr2) and Ge atoms represent the 6*g* plane. The crystal structure can be viewed as stacking of two different *xy* planes (planes containing the 4*d* and 6*g* sites) alternately stacked along the *c* axis. The rare-earth atoms have different occupancies at 4*d* and 6*g* crystallographic sites. The nearest-neighbor 4*d*-4*d* interatomic distance is 3.343 Å which is appreciably shorter than that corresponding 6*g*-6*g* atomic distance of 4.005 Å.[1] The interlayer (4*d*-6*g*) atomic distance is at an intermediate value of 3.758 Å.[1]

A. Pr_5Ge_3

Figure 3(a) shows the magnetization vs temperature curve for Pr_5Ge_3 under zero-field-cooled (ZFC) and field-cooled (FC) conditions with applied low fields of 20, 40, and 100 Oe along the $[10\bar{1}0]$ direction. Signatures of two magnetic transitions at $T_1 \approx 13$ K and $T_2 \approx 36$ K are seen in all the three fields. The upturn in the magnetization near T_2 suggests the onset of ferromagnetic correlations in the *ab* plane, while the transition at 13 K appears to have an antiferromagnetic character. Its position is independent of the applied field while the peak at higher temperature (corresponding to T_2 transition) broadens and shifts considerably to lower temperatures as the field is increased from 20 to 100 Oe. Thermomagnetic irreversibility under ZFC and FC conditions is observed for the transition at 36 K, which typically occurs in ferromagnets with large magnetocrystalline anisotropy. The latter also explains the peak shift to lower temperatures with increasing field as arising from an interplay of the applied and coercive fields. Between T_1 and T_2 the FC magnetization decreases in a limited range as the temperature is decreased at all fields, which is different from the typical saturation behavior of magnetization observed in ferromagnet in the FC mode.

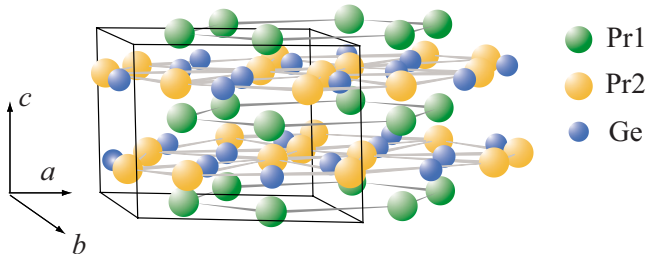

FIG. 2. (Color online) Crystal structure of the Pr_5Ge_3 compound: the black-lined edges represent the unit cell. The top, bottom, and central planes containing only Pr1 atoms represent the 4*d* planes and the remaining planes containing Pr2 and Ge atoms represent the 6*g* planes.

The magnetization with field parallel to the [0001] axis is shown in Fig. 3(b). There is only one magnetic transition at ≈ 13 K that is in contrast to that with field parallel to $[10\bar{1}0]$. The nature of the transition seems to be ferromagnetic but the negative magnetization in the ZFC condition indicates an overall ferrimagneticlike behavior. In the above measurements we have ensured that the notional zero fields in which the sample was cooled is not negative such that the negative ZFC magnetization is not attributed to a large coercive field. This transition seems to be the analog of that appearing along the $[10\bar{1}0]$ direction at ≈ 13 K but the behavior is totally different. The high-field (3 kOe) susceptibility curve is shown in Fig. 4(a). Along the $[10\bar{1}0]$ direction the T_2 peak has broadened appreciably to the point of becoming almost imperceptible; however, the low-temperature peak T_1 is

TABLE I. Refined crystallographic parameters for Pr_5Ge_3.

Atom	Site symmetry	*x*	*y*	*z*	U_{eq} (Å^2)	Occu.
Pr1	4*d*	0.333	0.666	0.000	0.269(2)	1
Pr2	6*g*	0.230(1)	0.000	0.250	2.218(4)	1.5
Ge	6*g*	0.604(6)	0.000	0.250	0.051(1)	1.5

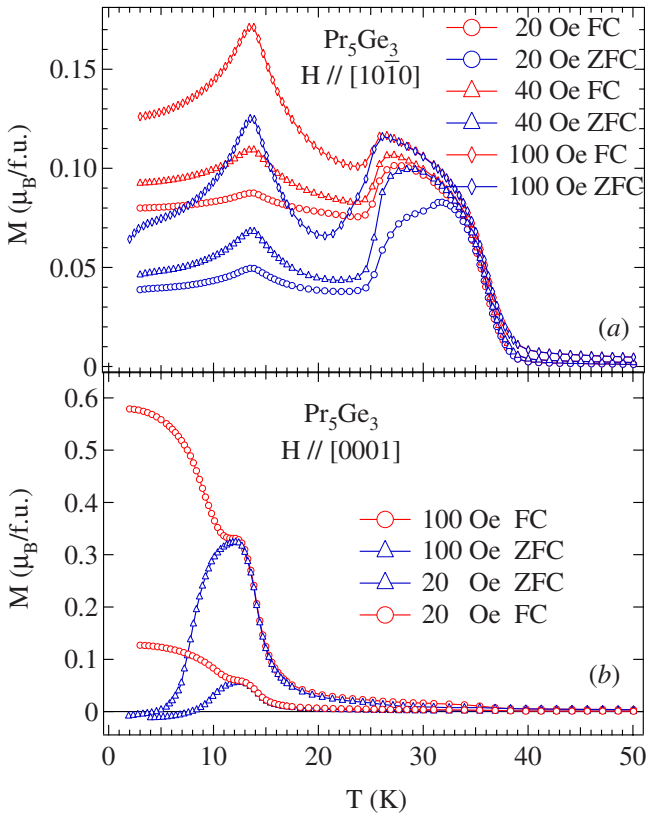

FIG. 3. (Color online) (a) Magnetization vs temperature curves for Pr_5Ge_3 with field parallel to $[10\bar{1}0]$. (b) Similar curves with field parallel to [0001].

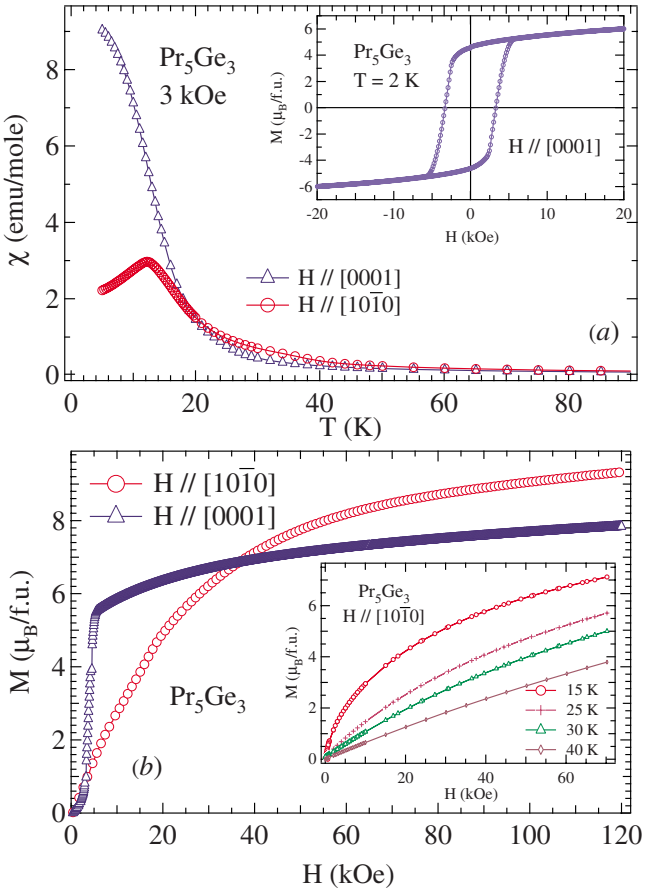

FIG. 4. (Color online) (a) High-field susceptibility of Pr_5Ge_3 along the $[10\bar{1}0]$ and [0001] directions with the inset showing the magnetic isotherm at 2 K with field along the [0001] direction. (b) Magnetic isotherms for Pr_5Ge_3 at 2 K along both the directions; the inset shows the field variation in magnetization along the $[10\bar{1}0]$ direction at a few selected temperatures.

clearly seen. On the other hand the magnetization along the [0001] direction shows a ferromagnetic ordering. The magnetic isotherms at 2 K for Pr_5Ge_3 with field along [0001] and $[10\bar{1}0]$ are shown in Fig. 4(b) with the inset showing the magnetic isotherms at 40, 30, 25, and 15 K along the $[10\bar{1}0]$ direction. The plots with the field along $[10\bar{1}0]$ show that overall the magnetization increases as the temperature is decreased, attaining substantial values at high fields. Overall the behavior for $T \leq 30$ K appears to be a superposition of both ferromagnetic and antiferromagnetic components. In particular focusing our attention on the 2 K plot the magnetization initially increases linearly with field and then moves toward saturation at high fields. The magnetization at low fields is less then that along the [0001] direction, but it overtakes the latter at ≈37 kOe and remains higher up to the highest applied field of 120 kOe. The magnetization at 120 kOe is $\approx 9.3 \mu_B$/f.u. In the reverse direction, the magnetization exhibits a hysteresis with a coercive field of ≈1 kOe (not shown). Along the [0001] direction the magnetization increases sharply with field as expected for a ferromagnetic compound and exhibits a hysteresis with a coercive field of 3.3 kOe as shown in the inset of Fig. 4(a). The magnetization at 120 kOe is $\approx 7.8 \mu_B$/f.u.

In order to get more information on the complex magnetic phenomenon revealed by dc magnetization data as presented above, we measured the ac susceptibility of the compound with an ac field applied along the two crystallographic directions $[10\bar{1}0]$ and [0001], respectively, as shown in Fig. 5. When the ac field is parallel to the $[10\bar{1}0]$ direction, the real part of the ac susceptibility (χ') shows peaks at approximately 36 and 13 K, whereas the imaginary part of the ac susceptibility (χ'') shows a peak only at 36 K. A peak in χ' reflects any type of magnetic ordering, whereas a peak in χ'' appears only if a ferromagnetic component is present. Hence a collinear antiferromagnetic ordering will not reflect in the imaginary part of the ac susceptibility. The presence of peak in both χ' and χ'' at 36 K indicates a magnetic ordering with net ferromagnetic component, whereas the absence of peak in χ'' at 13 K indicates a collinear type of antiferromagnetic ordering. This also supports our dc magnetization results where magnetization under FC and ZFC conditions bifurcates only at the T_2 transition. It may be noted that the peak at 13 K in χ' is stronger than that at the higher temperature. The increase in χ'' at low temperatures below approximately 8 K is presently not understood. When the ac field is applied along the [0001] direction, both the real and imaginary parts show a peak at approximately 13 K, consistent with the dc magnetization results, which show the dominant ferromagnetic behavior of the compound along this direction.

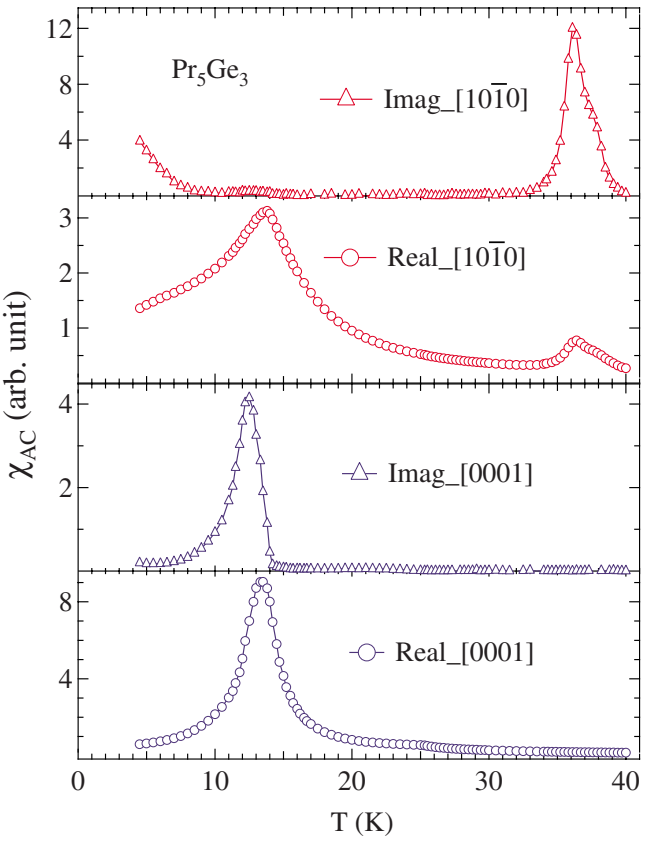

FIG. 5. (Color online) ac susceptibility of Pr_5Ge_3 with an ac field along the [10$\bar{1}$0] and [0001] directions.

The inverse susceptibility of the compound along the two directions is shown in Fig. 6. The solid lines are fits of the Curie-Weiss law to the data and furnish θ_P=16 K, μ_{eff} =3.58μ_B/Pr and θ_P=−10 K, μ_{eff}=3.58μ_B/Pr along the [10$\bar{1}$0] and [0001] directions, respectively. In the paramagnetic state the susceptibility along the [10$\bar{1}$0] direction is higher than that along [0001] at high temperatures, but at low temperature the susceptibility along [0001] is higher because of the ferromagnetic type of ordering [Fig. 4(a)]. It must be

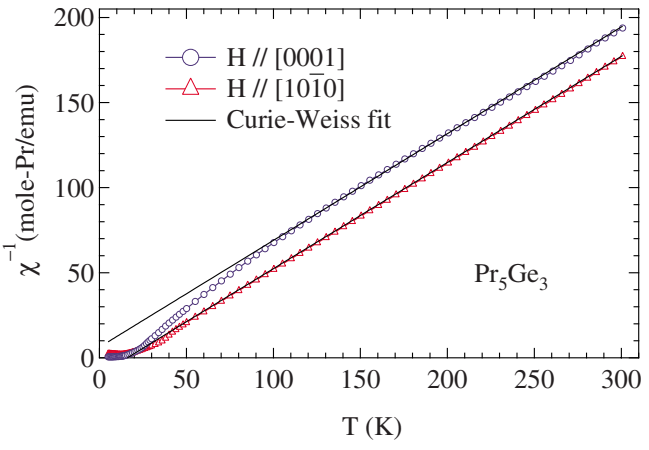

FIG. 6. (Color online) Inverse susceptibility of Pr_5Ge_3 with a Curie-Weiss fit.

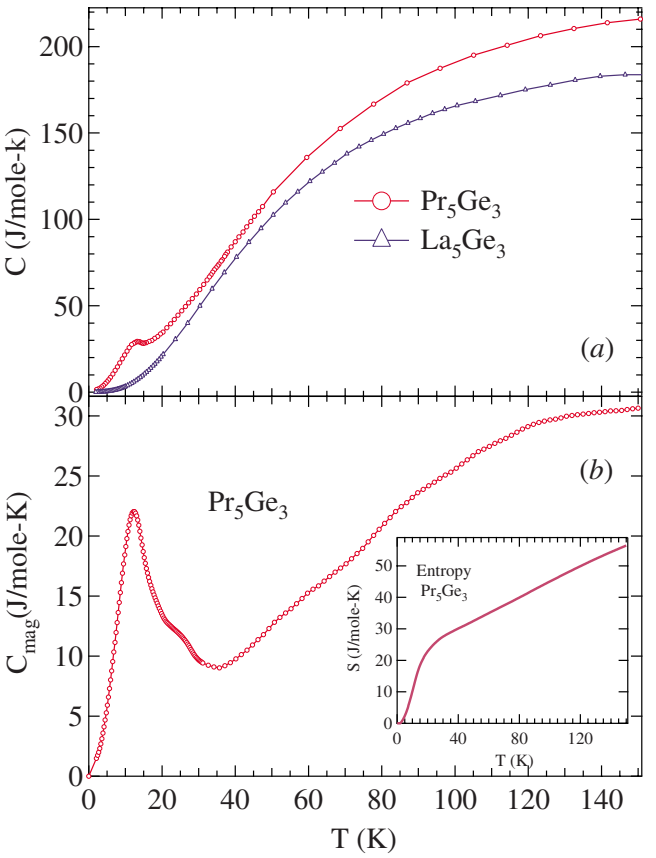

FIG. 7. (Color online) (a) Comparison of the heat capacity of Pr_5Ge_3 and La_5Ge_3. (b) The 4f contribution to the heat capacity of Pr_5Ge_3 with the inset showing the calculated entropy.

noted that the inverse susceptibility along the [0001] direction deviates from the Curie-Weiss fit at much higher temperature (100 K) than along the [10$\bar{1}$0] direction, indicating a dominant crystal-field effect for magnetization along the c axis. The high-temperature susceptibility and the magnetic isotherms at 2 K show that the easy axis of magnetization in Pr_5Ge_3 is along the ab plane.

The heat capacity of Pr_5Ge_3 and the nonmagnetic polycrystalline reference compound La_5Ge_3 is depicted in Fig. 7(a). The heat capacity of La_5Ge_3 increases monotonically with temperature as expected for a nonmagnetic compound. The heat capacity of Pr_5Ge_3 shows a minor peak at ≈13 K and then increases with an increase in temperature. Above 50 K the difference between the heat capacity of Pr_5Ge_3 and La_5Ge_3 increases, for which a likely reason could be that the presence of Schottky contribution arising from the Boltzmann fractional occupation of the thermally excited crystal electric field split levels in Pr_5Ge_3 or La_5Ge_3 may cease to be a good reference for the lattice heat capacity at high temperatures. Some evidence for the former comes from the fact that the high-temperature part (above 100 K) of the heat capacity of Pr_5Ge_3 could not be fitted to the sum of electronic (γT) and lattice contributions (Debye integral) alone. The 4f contribution to the heat capacity (C_{4f}) of Pr_5Ge_3 [Fig. 7(b)] was isolated by subtracting the heat capacity of La_5Ge_3, taking into account the slightly differing atomic masses of La and Pr. The peak at 13 K is now sharper in agreement with the

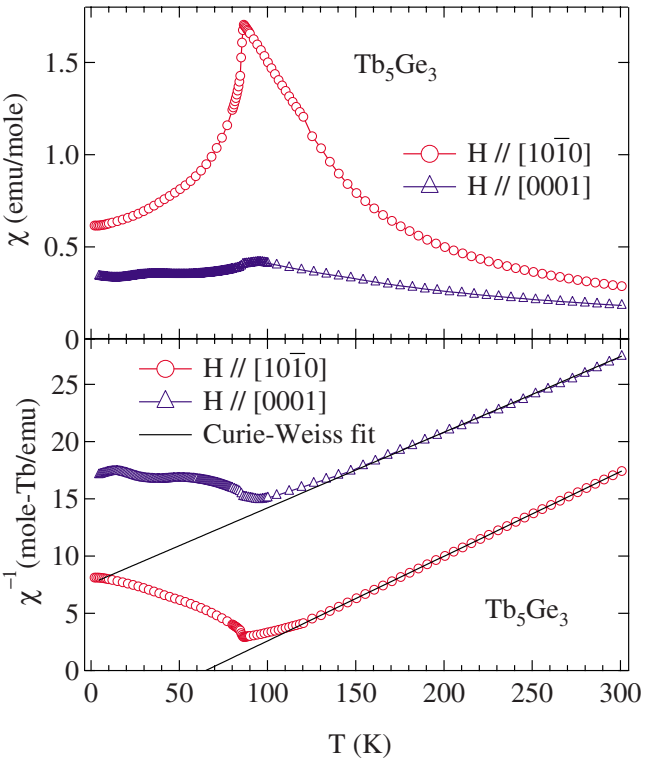

FIG. 8. (Color online) (a) Magnetic susceptibility of Tb_5Ge_3 along both the crystallographic directions. (b) Inverse magnetic susceptibility; the solid line through the data point indicates the Curie-Weiss fit.

magnetic ordering along both the crystallographic axes as deduced from the magnetization data above. There is no apparent anomaly at 36 K but a broad hump centered at ≈25 K is seen. We believe that the magnetic contribution to the heat capacity around 36 K may get submerged under the overriding Schottky anomaly which appears to be present as inferred from the upturn in the $4f$ heat capacity beginning at $T \approx 35$ K. The entropy calculated from C_{4f} is 3.2 and 6.3 J/mol K Pr at 13 and 40 K, respectively, compared to the value 5.76 J/mol K Pr for a doublet ground state. This shows that a substantial short-range order exists above 13 K. The T_2 peak in the magnetization along [10$\bar{1}$0] and the hump in the heat capacity may be a signature of the short-range order.

B. Tb_5Ge_3

The susceptibility of Tb_5Ge_3 with field applied along the crystallographic directions is shown in Fig. 8(a). The susceptibility with field parallel to the [10$\bar{1}$0] direction exhibits a sharp peak at the T_N=85 K characteristic of an antiferromagnetic transition. The susceptibility with field parallel to [0001] shows a kink at ≈85 K followed by a broad hump at low temperatures (between 20 and 50 K), indicating a relatively complex behavior. The inverse susceptibility is plotted in Fig. 8(b). In the paramagnetic region the fit of the Curie-Weiss law to the data furnishes θ_P=62 K, μ_{eff}=9.75μ_B/Tb and θ_P=−140 K, μ_{eff}=9.6μ_B/Tb along the [10$\bar{1}$0] and

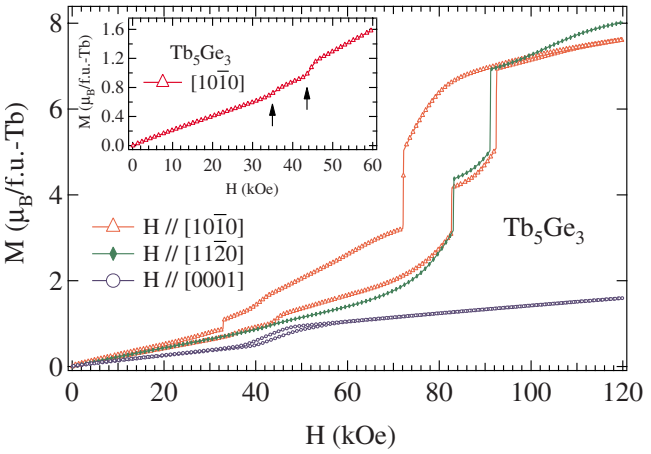

FIG. 9. (Color online) Magnetic isotherm of Tb_5Ge_3 with field along the [10$\bar{1}$0], [0001], and [11$\bar{2}$0] directions. The inset shows the expanded magnetic isotherm at low field with arrows pointing the metamagnetic transitions.

[0001] directions, respectively. The magnitude of the susceptibility along the two axes reflects the highly anisotropic magnetic response and also shows that [10$\bar{1}$0] is the easy direction of magnetization.

Figure 9 shows the magnetic isotherm of Tb_5Ge_3 with field along the [10$\bar{1}$0], [0001], and [11$\bar{2}$0] (lies within the *ab* plane) directions at 2 K. We have applied fields up to 120 kOe which exceed significantly the maximum applied field of 50 kOe used by Tsutaoka *et al.*[4] As a result we see extra features in the magnetization at high fields. The magnetization along the [10$\bar{1}$0] direction undergoes multiple metamagnetic transitions at ≈34, 42, 82, and 92 kOe. The former two magnetic transitions are spin-flip-like where as the latter two are spin-flop-like. The curved nature of the magnetic isotherm between approximately 60 and 80 kOe in the increasing direction of the field suggests a canted configuration of the antiferromagnetic state (AF II) (Fig. 10). The maximum magnetization at 120 kOe is ≈7.5μ_B/Tb, which is a little

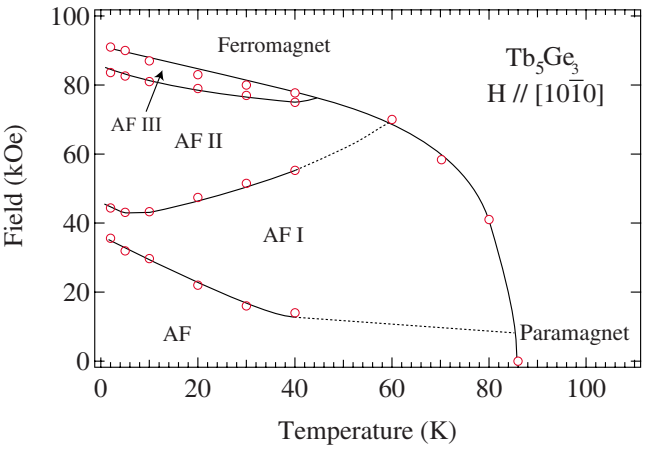

FIG. 10. (Color online) Magnetic phase diagram of Tb_5Ge_3 constructed using the temperature variation in magnetic isotherms with field applied along the [10$\bar{1}$0] direction. The dotted lines represent the expected imaginary path of the curve.

less than the saturation moment of the Tb^{3+} ion. Hence the latter two metamagnetic transitions drive the compound to the field-induced ferromagnetic state. A significant amount of hysteresis is observed during the demagnetization of the sample due to the pinning of the domain walls in an anisotropic ferromagnetic material. The field-induced ferromagnetic state of the compound indicates the weakly coupled antiferromagnetic nature of the compound. The magnetization along the hard axis undergoes a minor metamagnetic transition at ≈40 kOe. This result is in contrast to that reported previously,[4] where no metamagnetic transition is encountered up to a field of 50 kOe. The magnetization at 120 kOe and 2 K is $\approx 1.8\mu_B$/Tb, which is far less compared to that obtained with field along the $[10\bar{1}0]$ direction, as expected for a hard axis of magnetization. When the field is applied along the $[11\bar{2}0]$ direction the magnetization undergoes two spin-flop-like metamagnetic transitions at approximately the same values as that with field along the $[10\bar{1}0]$ direction. The magnetization at 120 kOe and 2 K is $\approx 8\mu_B$/Tb, which is $\approx 0.5\mu_B$/Tb higher then that along the $[10\bar{1}0]$ direction and close to the saturation moment of the Tb^{3+} ion. The magnetic phase diagram of the compound constructed from the temperature variation in the magnetic isotherms (not shown) with field applied along the easy axis of magnetization $[10\bar{1}0]$ is shown in Fig. 10. The symbols AF, AF I, AF II, and AF III represent the three different antiferromagnetic states (including the canted antiferromagnetic state) of the compound.

IV. DISCUSSION

In Secs. I–III we have presented the interesting magnetic behavior of Pr_5Ge_3 and Tb_5Ge_3. Pr_5Ge_3 orders ferrimagnetically near 13 K with a dominant ferromagnetic component when the field is applied along the [0001] direction. Along the $[10\bar{1}0]$ direction there are two transitions at T_1 and T_2; the transition at T_1 appears to be antiferromagnetic, while the upturn occurring at the higher temperature T_2 suggests the presence of ferromagneticlike correlations. At high fields the behavior of 2 K isotherms along both the crystallographic axes is dominantly ferromagneticlike. Since there are two symmetry inequivalent crystallographic sites, 4*d* and 6*g*, for the rare-earth ion and the nearest-neighbor 4*d*-4*d* distance that are significantly lesser than the corresponding 6*g*-6*g* distance, site-dependent magnetic response is in principle possible. The latter is actually seen in the neighboring (similar lattice parameters) isostructural compound Nd_5Ge_3 as mentioned in Sec. I. In Pr_5Ge_3 the behavior of the magnetization around ≈36 K with field along the $[10\bar{1}0]$ direction, which bears the signature of the onset of the ferromagneticlike correlations, can plausibly be attributed to the ions present at the 4*d* site. The 4*d* site moments being relatively closer to each other compared to the other ions are coupled more strongly by the indirect Ruderman-Kittel-Kasuya-Yoshida (RKKY) exchange interaction. With further decrease in the temperature the second magnetic transition at ≈13 K may be due to the *ab*-plane-projected collinear antiferromagneticlike ordering of the Pr^{3+} moments at the 6*g* site. As already mentioned above, the latter is strongly suggested by the ac susceptibility. The χ' (real part) of the ac susceptibility includes contributions from both magnetic rotation and domain-wall movement, whereas χ'' (imaginary part) reflects the energy loss due to the movement of domain walls. If the antiferromagnetic ordering is collinear then the resulting moment is zero and hence no movement of domain walls is involved, resulting in the absence of peak in χ''. We further speculate that between T_1 and T_2, the evolution of 4*d*-4*d*, 4*d*-6*g*, and 6*g*-6*g* interactions with temperature is such that it overall gives rise to a decrease in the FC magnetization in a limited range of temperature, as already mentioned above.

Along the [0001] direction, the peak seen in both the real and the imaginary parts of the ac susceptibility supports the ferromagnetic nature of the transition at 13 K, in tune with the dc magnetization results presented above. The relatively sharp nature of the peak is typically seen in highly anisotropic magnetic compounds, corroborated by the high coercivity (≈3 kOe at 2 K) seen in the magnetic isotherm.

The magnetic isotherms along the $[10\bar{1}0]$ and [0001] directions at 2 K show that at high fields Pr_5Ge_3 is like a ferromagnet. At 2 K the moment at 120 kOe is $\approx 9.3\mu_B$/f.u. and $7.8\mu_B$/f.u. along these two directions, respectively. Keeping in mind that the saturation moment of free Pr^{3+} ion is $3.2\mu_B$ and the likely reduction in the moment due to the crystal electric fields, the magnetization response involves the polarization of Pr ions of both sublattices. Of course, the magnetization along $[10\bar{1}0]$ is larger because it is the easy axis of magnetization.

The absence of any anomaly at 36 K when the field is applied along the [0001] axis may be rationalized by assuming that the easy axis of magnetization for the Pr 4*d* moments is in the *ab* plane. As the temperature is lowered a dominant ferromagnetic component is observed at ≈13 K with an overall ferrimagnetic behavior. Since the ordering temperature (≈13 K) is similar to that occurring also along the $[10\bar{1}0]$ direction, it is possible that the orientation of the 6*g* moments is such that it can be resolved into a collinear antiferromagnetic configuration in the *ab* plane and a ferromagnetic component along the *c* axis. In order to explain the ferrimagnetic response at low temperatures, we postulate that (i) the anisotropy of the 6*g* sublattice is stronger than that of 4*d* sublattice and (ii) the exchange interaction between the 6*g* and the 4*d* moments forces the latter to reorient from their easy axis. In order to get the full details of the magnetic configuration, neutron diffraction on a single crystal is required. The arrangement of the magnetic moments in these compounds can be very complex. For example, a recent neutron-diffraction experiment on Ho_5Ge_3 (Ref. 5) finds between $T_{N1}=27$ K and $T_{N2}=18$ K a sine-modulated ordering with two propagation vectors $K_1=[0,0,\pm 3/10]$ and $K_2=[0.1/2,0]$. The magnetic configuration changes below T_{N2} and is described by four propagation vectors $K_1=[0,0,\pm 3/10]$, $K_2=[0,1/2,0]$, $K_3=[0,0,\pm 2/5]$, and $K_4=[\pm 1/5,\pm 1/5,0]$.

Tb_5Ge_3, by contrast, shows a relatively simpler process of magnetic ordering. A peak at $T_N=85$ K is seen in both directions, though it is far more prominent along $[10\bar{1}0]$ (*ab*

plane), which is the easy axis of magnetization. The leveling of the susceptibility at low temperatures along the $[10\bar{1}0]$ direction may be due to the incommensurate magnetic transition reported[6] to occur between 75 and 50 K, which transforms into a spiral-like antiferromagnetic structure at low temperatures. The compound is a weakly coupled antiferromagnet in the sense that polycrystalline average of the paramagnetic Curie temperature is low (−16 K), and also the compound undergoes a field-induced ferromagnetic transition at 2 K. The saturation moment obtained at 120 kOe and 2 K is close to that reported from the neutron diffraction[6] for the Tb^{3+} ion in Tb_5Ge_3. Along the hard axis of magnetization there is an evidence of a metamagnetic transition at ≈40 kOe. Such transitions along the hard axis of magnetization are generally attributed to the crossing over of the crystal-field split energy levels as shown in case of $NdRhIn_5$.[7] The reason for hysteresis appearing in the magnetic isotherm is not known.

V. CONCLUSIONS

In conclusion, we have studied the magnetic properties of single-crystalline Pr_5Ge_3 and Tb_5Ge_3. The hexagonal *ab* plane or $[10\bar{1}0]$ direction was found to be the easy axis of magnetization for Pr_5Ge_3. In the *ab* plane, the magnetization shows a ferromagneticlike upturn at ≈36 K followed by a collinear antiferromagnetic ordering of the moments at ≈13 K. Along the [0001] direction the compound shows a dominant ferromagnetic transition at ≈13 K with an overall ferrimagneticlike behavior. At 2 K, the magnetic isotherm of the compound along the [0001] direction is typical for a ferromagnet, while a field-induced ferromagneticlike response is observed along the $[10\bar{1}0]$ direction. Tb_5Ge_3 was found to order antiferromagnetically at 85 K with the easy axis of magnetization laying in the *ab* plane. The compound undergoes a field-induced ferromagnetic state at low temperatures along the easy axis of magnetization.

[1] K. H. J. Buschow and J. F. Fast, Phys. Status Solidi **21**, 593 (1967).
[2] P. Schobinger-Papamantellos and K. H. J. Buschow, J. Magn. Magn. Mater. **49**, 349 (1985).
[3] M. Kurisu, T. Mitsumata, and I. Oguro, Physica B **259**, 96 (1999).
[4] T. Tsutaoka, Y. Nishiume, and T. Tokunaga, J. Magn. Magn. Mater. **272**, E421 (2004).
[5] A. V. Morozkin, O. Isnard, P. Henry, and P. Manfrinetti, J. Alloys Compd. **464**, 219 (2008).
[6] P. Schobinger-Papamantellos, J. Magn. Magn. Mater. **28**, 97 (1982).
[7] N. V. Hieu, T. Takeuchi, H. Shishido, C. Tonohiro, T. Yamada, H. Nakashima, K. Sugiyama, R. Settai, T. D. Matsuda, Y. Haga, M. Hagiwara, K. Kindo, S. Araki, Y. Nozue, and Y. Onuki, J. Phys. Soc. Jpn. **76**, 064702 (2007).